Ferroelectric domain structures in <001>-oriented $K_{0.15}Na_{0.85}NbO_3$ lead-free single crystal

Cite as: AIP Advances **5**, 037117 (2015); https://doi.org/10.1063/1.4914936
Submitted: 21 August 2014 . Accepted: 03 March 2015 . Published Online: 10 March 2015

Yan Chen, Chi-Man Wong, Hao Deng, Hei-Man Yau, Danyang Wang, Zhibo Yan, Haosu Luo, Helen L. W. Chan, and Jiyan Dai

Ferroelectric domain structures in <001>-oriented $K_{0.15}Na_{0.85}NbO_3$ lead-free single crystal

Yan Chen,[1,2] Chi-Man Wong,[1,2] Hao Deng,[3] Hei-Man Yau,[1,2]
Danyang Wang,[4] Zhibo Yan,[2] Haosu Luo,[3] Helen L. W. Chan,[2]
and Jiyan Dai[1,2,a]

[1]*The Hong Kong Polytechnic University Shenzhen Research Institute, Shenzhen, China*
[2]*Department of Applied Physics, The Hong Kong Polytechnic University, Hong Kong, China*
[3]*Information Materials and Devices Research Center, Shanghai Institute of Ceramics, Chinese Academy of Science, Shanghai, 201800, China*
[4]*School of Materials Science and Engineering, The University of New South Wales, Kensington, NSW 2052, Australia*

(Received 21 August 2014; accepted 3 March 2015; published online 10 March 2015)

In this work, ferroelectric domain structures of <001>-oriented $K_{0.15}Na_{0.85}NbO_3$ single crystal are characterized. Transmission electron microscopy (TEM) observation revealed high-density of laminate domain structures in the crystal and the lattices of the neighboring domains are found to be twisted in a small angle. Superlattice diffraction spots of $1/2\{eeo\}$ and $1/2\{ooe\}$ in electron diffraction patterns are observed in the crystal, revealing the $a^+a^+c^-$ tilting of oxygen octahedral in the perovskite structure. The piezoresponse of domains and *in-situ* poling responses of $K_{0.15}Na_{0.85}NbO_3$ crystal are observed by piezoresponse force microscopy (PFM), and the results assure its good ferroelectric properties. [http://dx.doi.org/10.1063/1.4914936]

INTRODUCTION

Lead zirconate titanate ($Pb(Zr_{1-x}Ti_x)O_3$ (PZT) ceramics are the most extensively used piezoelectric materials because of their good piezoelectric properties. However, the fabrication and application of the lead-based materials would give rise to serious environment problems. Thus, lead-free piezoelectric materials have been drawn much attention due to their environment friendly.[1,2] $K_xNa_{1-x}NbO_3$-based (KNN) system is considered as one of the most promising candidates of lead-free piezoelectric owing to its good ferroelectric properties and high Curie temperature (T_c =420°C).[2–4] A lot of investigations have been focusing on modifying the piezoelectric properties of KNN ceramics by doping metal ions, introducing perovskite oxides to form new solid solution and adopting different sintering methods such as hot pressing and spark plasma.[5] Besides KNN ceramics, the KNN-based single crystals have been grown to further improve the piezoelectric properties, because single crystals can be poled along different directions by domain engineering method.[6–9] The behavior of a ferroelectric is mainly dependent on the local domain response by applying an electrical loading. Therefore, the domain structures are very important for investigating the ferroelectric performance of the single crystal.

PFM is a powerful tool to directly observe the local ferroelectric domain structure of ferroelectric materials at nanoscale, and it can also probe local pizeoelectric property by measuring the so-called butterfly hysteresis loop.[10,11] TEM is a useful way to investigate the local structures, such as imaging the domain patterns and simultaneously revealing the crystallographic details by electron diffraction.[12,13] Most studies of the domain morphology characterization have been aimed at KNN-based ceramics using PFM[14,15] and TEM techniques.[15–18] Unfortunately, there were few

[a]Author to whom correspondence should be addressed; E-Mail: jiyan.dai@polyu.edu.hk

reports to investigate the detailed local structures, such as the domain morphology and domain boundary, of the KNN single crystal.

In this work, in order to better understand the domain structure of the KNN single crystal, its domain structures were characterized by PFM and TEM. Besides, the amplitude-voltage butterfly loop and phase-voltage loop were also evaluated.

EXPERIMENTS

The good-quality $K_{0.15}Na_{0.85}NbO_3$ single crystal was successfully grown using top-seeded solution growth method in Shanghai Institute of Ceramics. High purity carbonate and oxide powders, Na_2CO_3, K_2CO_3, Nb_2O_5 were used as starting materials. And the starting materials were weighted according to the chemical formula $K_{0.15}Na_{0.85}NbO_3$. The ferroelectric domains, as well as the butterfly loop were characterized by means of piezoresponse force microscopy (Asylum, Cypher, Asylum Research). For preparing the PFM sample, the single crystal was grinded and polished to about 50 μm thick, and silver paint was used to paste one face of the sample on a metal disk for characterization. The bright-filed and high-resolution TEM images, as well as the selected area electron diffraction patterns were obtained by transmission electron microscopy (JEM-2100F). For preparing TEM sample, the <001>-oriented $K_{0.15}Na_{0.85}NbO_3$ single crystal was grinded and polished to 40 μm thick, and then the thin plate was dimpled to 10 μm (Gatan, Model 656) and Ar-ion milled with Gatan PIPS 691 to obtain electron transparent sample.

RESULTS AND DISCUSSIONS

TEM observation reveals that there are large amount of domain structures in the KNN crystal, and some typical laminate domain structures are shown Figure 1. It can be seen that, the laminate domains can be in parallel and perpendicular to each other as shown in Figs. 1(a) and 1(b), and the domain size is in the range of ~100 nm in width (but not uniform). These domains are usually 90 degree ferroelectric domains and the movement of domain walls under electric field is believed to be an important contribution to the piezoelectric effect of the crystal. Figure 1(c) shows another feature of domain structure of both parallel and perpendicular domains and a triangle shaped domain (area

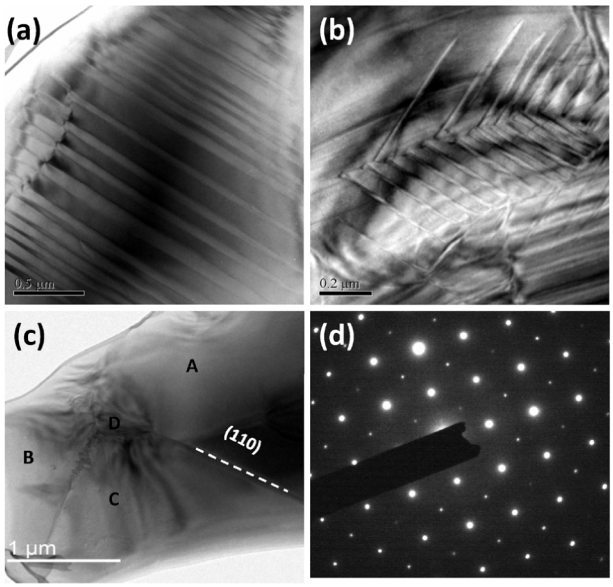

FIG. 1. (a-c) Low magnification TEM images of the KNN single crystal along <100> axes showing typical laminate domain structures, and (d) the corresponding selected area electron diffraction pattern.

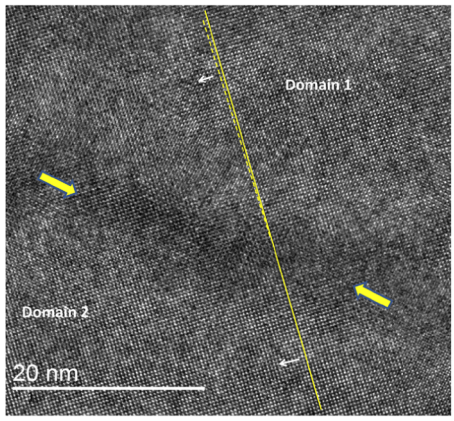

FIG. 2. High-resolution TEM image of two domains in the KNN single crystal.

D) surrounded by three domains (A, B and C). The domain walls are usually along the {110} planes (except the domain walls of B/D and C/D in Fig. 1(c)). A typical selected area electron diffraction (SAED) pattern representing most of the areas in the sample is shown in Fig. 1(d), which can be indexed as the diffraction along [001] zone axis with superlattice diffraction spots (will be discussed in the following session).

Figure 2 is a representative high-resolution TEM image of the domain wall structure showing two neighboring domains. Very careful exam of the image reveals that there is a very small angle lattice twist between the two neighboring domains; and the domain wall is along the {110} plane. Similar result was also observed in Ref. 19.

Figure 3 shows typical selected area diffraction patterns from different domains of the crystal along zone axes of <100>, where Figs. 3(a), 3(b), 3(c) and 3(d) are diffraction patterns obtained from the areas of A, B, C and D in Fig. 1(c), respectively. These diffraction patterns represent all possible superlattice diffraction spots in this KNN single crystal. Figure 3(a) shows the most representative diffraction pattern of the crystal, where the $^1/_2$(ooe) superlattice spots can be seen. It should be noticed that the four patterns in Fig. 3 showing different superlattice spots are very popular in this

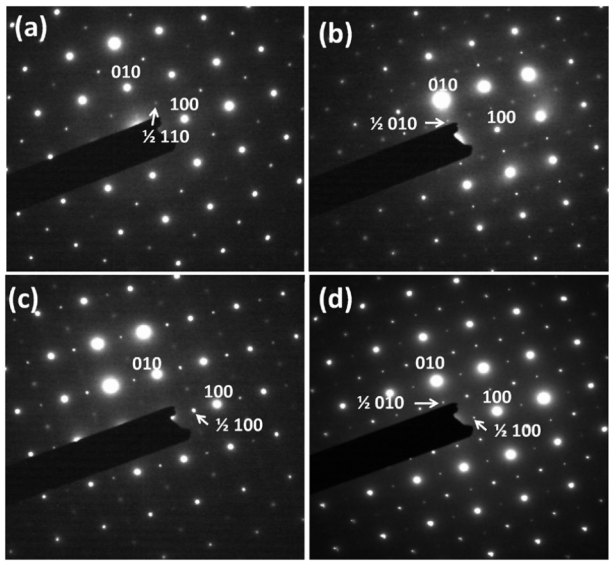

FIG. 3. (a-d) Typical selected area electron diffraction patterns of the KNN single crystal along from areas of A-D, respectively.

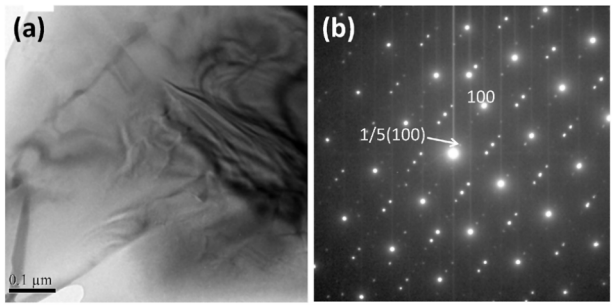

FIG. 4. (a) TEM image, and (b) the corresponding diffraction pattern, showing $\frac{1}{5}$ [100] supperlattice spots.

KNN crystal. When moving the electron beam around the crystal while taking the SAED, these four types of patterns change from one to the other. These four patterns can be indexed as <100> perovskite with supper spots of $^1/_2${eeo} and $^1/_2${ooe} superlattices. The superlattice points at $^1/_2$(100) and $^1/_2$(010) corresponds to the $\sqrt{2}$ax$\sqrt{2}$ax2a supercell. Referring to Table 8 of the Reaney's paper on tilting analysis with electron diffraction,[20] these four patterns should represent the $a^+a^+c^-$ tilting of oxygen octahedral viewed along different zone axes. We can see that the one with all superlattice reflections can be attributed to the [100] zone axis, and the one with only $^1/_2$(ooe) can be indexed as along the [001] axis. Therefore, we can conclude that the crystal is composed of domains oriented along all possible <100> directions. The existence of variants of [001], [100] and [010] domains in the crystal is favorable in reducing the strain of the crystal. Of course, tilting one pattern to a difference zone axis can confirm this, but it is not possible to tilt a single crystal to such large angle in TEM.

Another interesting phenomenon in this crystal is that, an area shows diffraction pattern with superlattice spots close to $\frac{1}{5}$(100) (but twisted a little from [100] direction) corresponding to 5 times lattice spacing (see Fig. 4(a) the morphology and (b) the corresponding diffraction pattern). Structures of antiferroelectric supercells of $\sqrt{2}$ax$\sqrt{2}$ax4a and $\sqrt{2}$ax$\sqrt{2}$ax6a supercells, as well as their incommnesrate structure have been reported in the KNN ceramics.[21] $NaNbO_3$ has an antiferroelectric phase with space group *Pbcm* at room temperature (300 K). The antiferroelectric phase consists of two or more sublattice polarizations of antiparallel nature, which in turn give rise to superlattice reflections in the diffraction patterns. However, the result shown in Fig. 4 is different from what has been reported the 4 and 6 times of lattice spaced antiferroelectric phases. One can also see that the superlattice spots oriented a few degrees away from the [100] direction. We believe that the appearance of the $\frac{1}{5}$ (100) superlattice is due to defect or impurity induced local incommensurate structure. It should be noticed, such diffraction pattern is not common in this crystal.

The ferroelectric domain characteristics of the crystal were also studied by PFM. Figure 5 shows typical PFM images of the KNN single crystal, where the isolated-island domain can be observed in Fig. 5(a) which is an unpoled area. Figure 5(b) presents the PFM image after locally poled by applying a dc bias (+10 V with 4 μm scan size and −10 V with 2 μm scan size). The dc bias causes domains switching, so that the different contrasts from the areas being positively

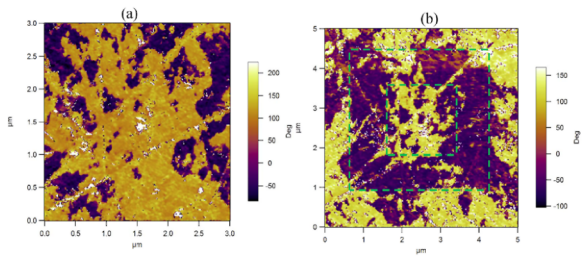

FIG. 5. PFM images of the domain structure for KNN single crystal: (a) before poling, and (b) after poling with a dc bias (+10 V with 4 μm scan size and −10 V with 2 μm scan size).

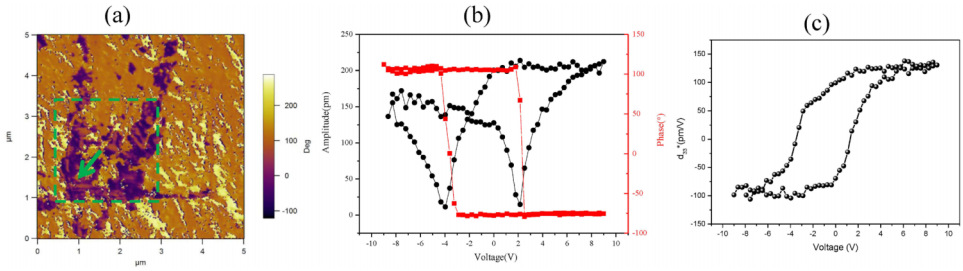

FIG. 6. (a) PFM image of the domain structure after poling with a DC bias (+10 V with 4 μm scan size and −10 V with 2 μm scan size) showing laminate domains, (b) amplitude-voltage butterfly loop and phase-voltage hysteresis loop, and (c) effective piezoelectric coefficient d_{33}^* - voltage hysteresis loop.

and negatively poled exhibit different polarization directions.[22] Unlike some other crystals which show sharp domain boundaries between the different polarized area, this KNN crystal shows very irregular domain boundaries. This may be due to the existence of unevenly distributed laminate domains and defect pinning to the movement of domain walls.

Figure 6(a) shows a PFM image with a DC bias (+10 V with 4 μm scan size and −10 V with 2 μm scan size) in a different location. Although the areas contrasts are not sharp, some small stripe-like and cross-like (the arrow) structure domains can be identified in the local poled area, which is different from the irregular and isolated-island domains shown in Fig. 5(a). These stripe-like and the cross-like domains can be relative to the laminate domain structure as given in TEM images shown in Fig. 1. The clear contrast of the domain structure in the PFM image suggests its contribution to piezoelectricity. Besides, the amplitude-voltage butterfly loop, phase-voltage and effective piezoelectric coefficient d_{33}^* - voltage hysteresis loop were investigated for further understanding the domain switching as shown in Figs. (6b-6c). An effective piezoelectric coefficient d_{33}^* of ~120 pm/V was observed from Fig. 6(c). The hysteresis loops confirms the domain switching without any sign of leakage behavior which indicates the good ferroelectric property of the KNN single crystal.

CONCLUSIONS

The ferroelectric domains and local structures of <001>-oriented $K_{0.15}Na_{0.85}NbO_3$ single crystal have been studied. Typical laminate domain structures and $a^+a^+c^-$ tilting of oxygen octahedral in the perovskite structure have been observed. Butterfly loop and phase-voltage hysteresis loop of the KNN single crystal suggest its good electric property.

ACKNOWLEDGMENTS

This research was supported by the National key Basic Research Program of China (973 Program) under Grant No. 2013CB632900. Financial support from The Hong Kong Polytechnic University strategic plan (No: 1-ZVCG&1-ZV9B).

[1] T. R. Shrout and S. J. Zhang, J. Electroceram. **19**, 111 (2007).
[2] Y. Saito, H. Takao, T. Tani, T. Nonoyama, K. Takatori, T. Homma, T. Nagaya, and M. Nakamura, Nature **432**, 84 (2004).
[3] E. Ringgaard and T. Wurlitzer, J. Eur. Ceram. Soc. **25**, 2701 (2005).
[4] H. L. Du, Z. M. Li, F. S. Tang, S. B. Qu, Z. B. Pei, and W. C. Zhou, Mater. Sci. Eng. B **131**, 83 (2006).
[5] H. L. Du, D. J. Liu, F. S. Tang, D. M. Zhu, W. C. Zhou, and S. B. Qu, J. Am. Ceram. Soc. **90**, 2824 (2007).
[6] X. Q. Huo, L. M. Zheng, S. J. Zhang, R. Zhang, G. Liu, R. Wang, B. Yang, W. W. Cao, and T. R. Shrout, Phys. Status Solidi RRL **8**, 86 (2014).
[7] L. M. Zheng, X. Q. Huo, R. Wang, J. J. Wang, W. H. Jiang, and W. W. Cao, CrystEngComm **15**, 7718 (2013).
[8] D. B. Lin, Z. R. Li, Z. Xu, and X. Yao, Ferroelectrics **381**, 1 (2009).
[9] Y. Noguchi and M. Miyayama, J. Ceram. Soc. Jpn. **118**, 711 (2010).
[10] S. V. Kalinin, A. Rar, and S. Jesse, IEEE Trans. Ultrason., Ferroelect., Freq. Control **58**, 249 (2011).
[11] Y. M. Liu, K. H. Lam, K. K. Shung, J. Y. Li, and Q. F. Zhou, J. Appl. Phys. **113**, 187205 (2013).
[12] C. W. Tai, S. H. Choy, and H. L. W. Chan, J. Am. Ceram. Soc. **91**, 3335 (2008).

[13] X. L. Tan, C. Ma, J. Frederick, S. Beckman, and K. G. Webber, J. Am. Ceram. Soc. **94**, 4091 (2011).
[14] F. Z. Yao, Q. Yu, K. Wang, Q. Li, and J. F. Li, RSC Adv. **4**, 20062 (2014).
[15] K. Wang, F. Z. Yao, W. Jo, D. Gobeljic, V. V. Shvartsman, D. C. Lupascu, J. F. Li, and J. Rödel, Adv. Funct. Mater. **23**, 4079 (2013).
[16] S. J. Zhang, H. J. Lee, C. Ma, and X. L. Tan, J. Am. Ceram. Soc. **94**, 3659 (2011).
[17] H. Z. Guo, S. J. Zhang, S. P. Beckman, and X. L. Tan, J. Appl. Phys. **114**, 154102 (2013).
[18] Y. Huan, X. H. Wang, Z. B. Shen, J. Y. Kim, H. H. Zhou, and L. T. Li, J. Am. Ceram. Soc. **97**, 700 (2014).
[19] J. J. Yao, Y.D. Yang, N. Monsegue, Y. X. Li, J. F. Li, Q. H. Zhang, W. W. Ge, H. S. Luo, and D. Viehland, Appl. Phys. Lett. **98**, 132903 (2011).
[20] D. I. Woodward and I. M. Reaney, Acta Crystallogr. Sect. B: Struct. Sci. **61**, 387 (2005).
[21] K. Kobayashi, M. Ryu, Y. Doshida, Y. Mizuno, and C. A. Randall, J. Am. Ceram. Soc. **96**, 531 (2013).
[22] Y. Chen, J. Y. Dai, K. Au, K. H. Lam, Y. B. Qin, and H. X. Yang, Mater. Lett. **68**, 54 (2012).